

SKELETONS, PERIODIC ORBITS AND SUPERSCARS IN THE RATIONAL POLYGON BILLIARDS AND ELSEWHERE

STEFAN GILLER

Jan Długosz University in Czestochowa, Institute of Physics
Armii Krajowej 13/15, 42-200 Częstochowa, Poland
stefan.giller@ajd.czest.pl

JAROSŁAW JANIĄK

Theoretical Physics Department II, University of Łódź
Pomorska 149/153, 90-236 Łódź, Poland
j.janiak@yahoo.pl

(Received April 22, 2013)

Semiclassical wave functions based on the Maslov–Fedoriuk approach and satisfying the Dirichlet boundary conditions are constructed in the rational polygon billiards. They are defined on classical objects called skeletons which are the billiard generalization of Arnold’s tori. The skeletons, which are considered, are built of periodic trajectories. In the phase space, these skeletons are represented by Lagrange surfaces which have forms of cylinder-like or Möbius-like bands. Semiclassical solutions constructed on these surfaces are *exact* making the Lagrange surface billiard-like. Projected on the rational polygon billiards these exact solutions become again semiclassical taking the forms of the superscars of Bogomolny and Schmit [*Phys. Rev. Lett.* **92**, 244102 (2004)]. This allows us to consider the exact solutions on the Lagrange surfaces as the resonant states for the rational billiards which manifest themselves in the form of superscars in the high energy limit. It is shown that the superscar states can be found also in the chaotic deformations of the polygon billiards such as the Bunimovich or Sinai ones.

DOI:10.5506/APhysPolB.44.1725

PACS numbers: 03.65.–w, 03.65.Sq, 02.30.Jr, 02.30.Lt

1. Introduction

Billiards while a non-analytic motion area are, however, well known as examples of the non-integrable two dimensional systems, except the known cases of the integrable elliptical, rectangular and some triangle billiards.

They are widely considered as a simple field of experimental [1–3] as well as theoretical [4–7] (and papers cited there) and computational investigations [8–10] allowing to apply many different methods (see Sarnak’s lecture [11] and [3] of the same author for an extensive review of the respective theoretical methods covering also billiard manifolds as well as the students book of Tabachnikov [12]).

In this paper, we are going to apply to the two-dimensional rational polygon billiards the semiclassical wave function (SWF) formalism developed in our earlier paper [13] and based on the well known Maslov–Fedoriuk approach. The latter was tailored respectively to the specific form of the billiard dynamics developed in the two-dimensional rational polygon billiards. The dynamics of such billiards has been called by Richens and Berry [8] (see also Tabachnikov [12]) pseudointegrable. It is interesting because of its position between the integrable dynamics and the chaotic ones.

A huge number of papers and monographs have been devoted already to studying both the classical and quantum dynamics of the rational polygon billiards both by mathematicians (see [12, 14] for the classical treatment of the problem from the mathematical point of view) and physicists including theoretical, computing and experimental works of the latter. However, even for these restricted kinds of the polygon billiards their dynamics seem to be still not well understood, for both the cases — the classical and the quantum billiards.

In the Maslov–Fedoriuk approach to the problem, however, it is not the dynamics of single trajectories, periodic or aperiodic ones, which is as much important but rather an existence and a corresponding dynamics of sets of such trajectories forming some closed systems, which in this paper are called skeletons. These are just the systems on which global semiclassical wave functions are constructed in the Maslov–Fedoriuk approach.

Let us note, at the moment, that a description “semiclassical” does not mean necessarily the limit $\hbar \rightarrow 0$, but also a limit of any quantity, such as the energy parameter, some parameters of potentials *etc.*, respective limit of which can be treated from the mathematical point of view by the methods developed by Maslov and Fedoriuk [15] and modified in our paper [13]. In the case of the billiard dynamics, the corresponding semiclassical parameter is, in the present paper, the energy the infinite limit of which corresponds, of course, to the short wave one.

Let us note further that the Maslov–Fedoriuk approach is quite general covering a very wide class of partial differential equations which includes also the Schrödinger one. Considering the latter and following Maslov and Fedoriuk, one concludes that all what is really needed to construct a global semiclassical solution to the Schrödinger equation (SE) in the rational polygon billiards (RPB) in the high energy limit is the following:

- realize that the dynamics in the RPB are just reflections of the billiard ball on the billiard boundary ruled by the geometrical optic laws, while the ball itself moves along a straight line (*ray*) between any two of its successive reflections (see below for a more precise description of this dynamics);
- construct, in the phase space corresponding to such a mechanics, a set of Lagrange surfaces (manifolds) (LS) [8, 16, 17] with the properties:
 - each LS is built of a finite set of congruences (Keller and Rubinov [17]);
 - each of the congruences of a LS contains a connected set of rays which are parallel to each other and begins and ends at the billiard boundary each;
 - each LS is built of congruences by gluing them on those of their boundaries which coincide with the billiard one [8, 17];
 - by the above gluing construction, each LS is *closed* for any of its rays, *i.e.* each ray of a LS can never leave it being reflected by the billiard boundary;
 - each Lagrange surface is maximal, *i.e.* it cannot be enlarged by additional congruences if conditions of the problem considered are to be satisfied;
- build on each of the constructed Lagrange surfaces two *basic* semiclassical solutions to the Schrödinger equation satisfying necessary conditions of continuity, uniqueness and boundary ones;
- project on the billiard area each particular Lagrange surface equipped with the two basic semiclassical wave functions (BSWF) defined on them. Note that a number of points of the Lagrange surface projected onto a single point of the billiards is finite in the RPB case;
- form a proper linear combination of the projected BSWFs in each point of the billiard area covered by the projected Lagrange surface. The constructed combinations must satisfy necessary conditions on the billiard boundary providing us in this way with a *global* SWF (GSWF) defined on the chosen Lagrange surface;
- put to zeros values of the GSWF in each point of the billiards not covered by the Lagrange surface projection to get in this way a semiclassical solution to the self energy problem in the billiards.

The result of the projection of a Lagrange surface on the billiard area is a set of trajectories called a *skeleton*. Congruences of a LS are projected into the billiards as *bundles*, so that each skeleton is built in a closed way of bundles of rays reflected by the billiard boundary [13].

Since constructions of skeletons seem to be easier than the respective Lagrange surfaces, the construction of the GSWF's described above can be substituted equivalently by their direct respective construction on skeletons. Namely, the BSWF's can be defined just first on the bundles while the GSWF's can be uniquely and continuously defined on the skeletons satisfying on them the boundary conditions of Dirichlet or Neumann becoming proper linear combinations of the BSWF's.

Constructing skeletons the following elementary rules which govern the rational polygon billiards (RPB) dynamics must be taken into account:

- each ray is reflected by the billiard boundaries according to the rules of geometrical optics making a finite number of different angles with the billiard edges;
- each ray runs along a straight line between its two successive reflections of the boundary;
- vertices of the polygon billiards are singular points for the billiard trajectory dynamics, *i.e.* at these points trajectories do not satisfy the optical reflection rule;
- each rational polygon billiard can be “unfolded” by successive mirror-like reflection operation in each pair of their two edges joined by the common vertex so that by a finite number of such operations the RPB comes back to its initial position;
- each ray runs along a straight line on the respectively unfolded billiards;
- if a trajectory is aperiodic, a set of points by which it is reflected is:
 - dense on the whole billiard boundary; or
 - dense on a subset of the billiard boundary while on the remaining parts of the boundary such points are absent at all depending on the trajectory;
- if a trajectory is periodic, the corresponding set of its reflection points is finite;
- a set of angles by which all periodic trajectories are reflected is dense on the segment $(0, \pi)$ [18];

- a periodic trajectory emerging from some vertex of the billiards, called by Bogomolny *et al.* [19, 20] a *singular diagonal* (SD) (while mathematicians called it a *generalized diagonal* [18]), has to pass on its way by the same or other vertices;
- the set of all SD's is countable.

According to the above rules, skeletons in the Maslov–Fedoriuk approach can take several different forms providing us with the corresponding different forms of the GSWF's and their energy spectra. While we describe skeletons sufficiently fully in the next sections, let us note here that each bundle of a skeleton in the RPB contains only parallel segments of trajectories crossing the billiards between two successive reflections. Because of that, any skeleton in the RPB can contain only periodic or only aperiodic trajectories. Moreover, skeletons in the RPB differ from each other by the following properties of their bundles:

- each bundle of a skeleton covers by its trajectories the whole area of the billiards;
- none bundle of a skeleton has the property of the previous point.

In the first case, a skeleton is *global* but cannot contain periodic trajectories.

Singular skeletons of the second class can be built by periodic trajectories as well as by aperiodic ones. The aperiodic skeletons seem, however, to be strictly related with the periodic ones being their complements on the RPB area.

In the phase space, the corresponding Lagrange surfaces have forms of closed compact two-dimensional surfaces of some genus g in the case of the global skeletons.

For the singular skeletons, the Lagrange surfaces can take the forms of the cylinder-like or the Möbius-like bands, if they are built of periodic orbits or forms of the surfaces of a genus g with holes in them, if trajectories building them are aperiodic.

There is also another important difference between the skeletons of both the kinds. Namely, the global skeletons can exist, as it seems, at most in the pseudointegrable billiards, whereas the singular skeletons, which are strictly related to the existing periodic orbits in billiards, can be found not only in the rational polygon billiards but also in arbitrary billiards with respective parts of flat boundaries including billiards with chaotic motions. An example of the latter one is the Bunimovich stadium with its bouncing ball modes generated by the periodic orbit skeleton built between its two flat parallel parts of its boundaries.

Still another serious drawback related with the global skeletons which differs them from the singular ones and which can give rise for criticizing the Maslov–Fedoriuk approach at all, if it is applied to non-integrable systems such as the pseudointegrable ones, is that the global semiclassical wave functions which can be built on the global skeletons in such systems can provide us only with a part of the complete semiclassical solutions to the SE, *i.e.* some essential part of possible solutions with accompanied energy spectra can be unavailable by the method.

A reason for such a drawback lies, as it seems, in the semiclassical idea itself which introduces to the respective physics natural units of lengths, namely the wave lengths or their parts. As a result, linear dimensions of the quantum problems investigated in the semiclassical limit should be expressed naturally in the wave length units. If these dimensions are incommensurate in the wave length units, then some necessary conditions for the semiclassical wave functions, such as their continuity and boundary conditions, cannot be satisfied simultaneously in many problems.

In particular, using simultaneously the Dirichlet and the Neumann boundary conditions leads frequently to a conflict since if the first kind of the conditions needs linear dimensions to be measured by the half wave units, then the second needs the quarter wave ones. As a consequence, it is not possible, for example, to construct an even set of the semiclassical wave function for the rhombus built of the two equilateral triangles [8] or to demand both the conditions on different parts of the same edges of the polygon billiards.

An importance of the above notes on the global skeletons is related strictly with the common conviction that just these skeletons should be considered as the ones on which the semiclassical wave functions approximating the quantum billiard problems can be built. From this point of view, the existence of the singular skeletons and the corresponding semiclassical solutions built on them seems to be a little bit mysterious.

Therefore, in this paper, having in mind the above limitations of the M–F approach with constructing GSWF’s on the global skeletons, we devote our main attention to the singular semiclassical solutions existing in the RPB. Just these solutions seem to be the most interesting because of the recent both theoretical [19, 20] and experimental results [1, 2, 20–22] which, as it seems to us, provide us with a good opportunity for their physical interpretations by the singular semiclassical solutions built on periodic skeletons.

Namely, Bogomolny *et al.* [19, 20] (see also Bogomolny *et al.* [23]) have found, by a completely different way of analysis, that in the high energy limit the periodic trajectories existing in the rational billiards have to express themselves in the form of the superscars states. This conclusion has been obtained by the authors as a high energy limit result of the scattering of

the flat wave function on the infinite number of scattering centers regularly distributed along a straight line when the wave vector was almost parallel to the line [23]. This analysis was stimulated by considering the reflections of the ray bundles by vertices of the rational polygon billiards as the result of the scattering of the bundles on the vertices. It appears, however, that these high energy superscars states coincide exactly with the semiclassical wave functions built on the singular skeletons associated with the periodic orbits considered by Bogomolny *et al.* [19, 20].

On the other hand, the authors of the papers [1, 2, 20–22] confirmed experimentally the existence of the singular semiclassical states in the resonant cavities they investigated.

Since, as we have already mentioned, singular skeletons are typical not only for the rational polygon billiards but can be met also in the chaotic systems, then one can expect the existence of the superscar states also in such systems. Again, a well known example is the Bunimovich stadium with its bouncing ball modes [2, 4, 5]. However, one can easily give many other examples of the chaotic billiards with any form of the superscars which can be found in the broken rectangular billiards.

In this paper, we are going to show that the superscar states which can be defined on the singular skeletons are common in the RPB's but can be found also in every billiard a boundary of which satisfies some conditions of a geometrical nature. Namely, the boundary of such a billiard has to contain some elements of the RPB boundary so that the considered billiard can be substituted by a RPB preserving these elements.

However, our *main* result in explaining the mystery of the SWF's built on the periodic skeletons is establishing that they are perfectly regular and exact solutions of the Schrödinger equation on the Lagrange manifolds corresponding to these periodic skeletons developed in the billiards. Therefore, these *exact* states and their energy spectra can be considered as the virtual part of the real energy spectra of the respective billiards giving rise to the corresponding resonant effects [24] which manifest themselves as the superscar states in billiards in the high energy limit.

In fact, because of their abundance, Bogomolny *et al.* [19] suggested to use even the superscar solutions and their spectra as the approximations to the real solutions and the real energy spectra. However, as it was noticed in the recent paper by Marklof and Rudnick [25], the latter possibility cannot be realized.

The paper is organized as follows.

We begin by reminding shortly the idea of skeletons to get tools for the next sections.

In Sec. 3 the periodic skeletons of the simplest billiard, *i.e.* the rectangular one are considered to show the abundance of the singular periodic skeletons in this case, and the corresponding abundance of the superscar states. These states are shown to exist as the exact solutions to the SE on the Lagrange surfaces corresponding to the skeletons considered.

In the next section, the periodic skeletons are considered in the simplest case of the broken rectangular billiards. These billiards can be obtained by gluing together a finite number of rectangles. They can be considered as an archetype of the rational pseudointegrable polygon billiards since by a standard way of gluing the rectangles one can obtain the pseudointegrable billiards with any genus g of a Lagrange surface corresponding to it.

A variety of periodic skeletons, which can be easily found in the broken billiards considered, are discussed in these section and it is shown again a direct relation between the GSWF's built on the skeletons and their exact representations on the corresponding Lagrange surfaces whose shapes have the cylinder-like bands.

Also in this section, it is noticed that the periodic skeletons in the broken rectangular billiards are accompanied frequently by the complement skeletons the LS's of which are much more complicated having forms of surfaces with some genres but with additional holes in them.

In Sec. 5 the triangle and the pentagon billiards are considered. In this section, it is shown that shapes of the Lagrange surface can be also the Möbius-like closed bands and the exact solutions of the SE which can be found on the surfaces being projected on the respective billiards become the semiclassical superscar states.

Next in Sec. 6, it is shown that the superscar SWF's can be implemented into chaotic deformations of the rectangle, the broken rectangle, the triangle and the pentagon billiards. In Sec. 7 the results of the paper are summarized.

2. Skeletons and semiclassical wave functions in the rational polygon billiards

In this section, we shall sketch a description of the notion of a skeleton. The more complete and precise definition of it can be found in [13].

2.1. Rays, bundle of rays and skeletons — classical constructions in billiards

Consider a rational polygon billiard B_R shown in Fig. 1. It consists of N edges (sides) with all its angles being a rational part of π .

A trajectory which is shown in the figure emerges from the side $A_k A_{k+1}$ making an angle α_i with the side. The shadow area covers all the trajectories emerging from the segment $(u_i, u_i + l_i)$ of the length l_i and making all the

same angles α_i with the side A_k . These are rays of the bundle B_i . Each bundle is an open set of rays. Each bundle is totally defined on a given side of the RPB. Obviously, each bundle can contain parallel rays only.

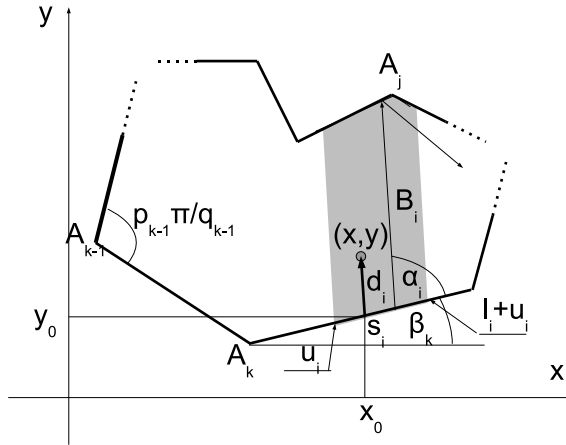


Fig. 1. An arbitrary rational polygon billiard B with a bundle B_i .

A bundle B_i can be totally reflected off by a single side only or by two or more sides as it is shown in Fig. 1. In the latter case, it is said to be scattered by the vertex A_j by which it is divided into two parts. Each of these two parts can belong to another bundles defined on the sides A_jA_{j+1} and $A_{j-1}A_j$.

Vertices of B_R are *singular* points for bundles reflecting on them, *i.e.* a reflection of a bundle ray passing by such a vertex can be undefined. Such a reflection can be, however, always uniquely defined if a bundle is a member of a skeleton.

A *skeleton* \mathbf{B} is a set of bundles B_i , $i = 1, \dots, n$, which is closed under reflections of its bundles on the B_R -boundary. It means that by such reflections each bundle of the skeleton is scattered into subsets of another bundles belonging to the skeleton \mathbf{B} . Therefore, a ray belonging to the skeleton cannot leave it by its subsequent reflections.

We shall assume that each skeleton satisfies the *mini-max* principle in the following meaning:

- it cannot be decomposed into another two or more disjoint subsets of its bundles forming new skeletons each; and
- it cannot be obtained by such a decomposition.

A *global* skeleton is the one, each bundle of which or respective unions of its bundles cover the billiard totally, excluding may be some sides of the B_R -boundary.

Skeletons which are not global are *singular*.

Global skeletons in B_R can be represented in the phase space by closed surfaces of definite genres g . Namely [8, 12, 14, 17],

$$g = 1 + \frac{C}{2} \sum_{k=1}^N \frac{p_k - 1}{q_k}, \quad (1)$$

where N is a number of the polygon vertices, $\pi \frac{p_k}{q_k}$ with coprime integers p_k , q_k is an angle enclosed k th vertex, $k = 1, \dots, N$, and C is the least common multiple of q_k .

Singular skeletons in B_R generated by periodic trajectories are represented in the phase space by closed cylinder-like or Möbius-like bands, while their complement skeletons (see Sec. 5.1) by surfaces of some genres with holes in them.

Trajectories which are not periodic and do not belong to any complement skeleton will be called *generic*.

We shall further *assume* that reflection points of each generic trajectory are densely distributed on the whole RPB boundary since such a property of the generic trajectories seems to be not firmly established.

We shall also *assume*, for the same reasons, that global skeletons can be built only by generic trajectories.

It is the RPB skeleton property that if it contains at least one periodic trajectory then all trajectories of such a skeleton are also periodic. In such a skeleton, there are always at most two periodic trajectories each of which starts from some vertex of the polygon and ends on the same vertex or on another.

These two periodic trajectories have been called *singular diagonals* (SD's) by Bogomolny and Schmit [19], while such a *periodic* skeleton itself has been called the *periodic orbit channel* (POC).

Therefore, each periodic skeleton is defined at most by two SD's.

A basic property of the periodic skeletons is that they are *never* scattered by any vertex, *i.e.* each bundle of such skeletons is totally reflected into another *single* bundle of the periodic skeletons. This is why in the phase space the Lagrange surface of the periodic skeletons have forms of the cylinder-like bands (in the case of two SD's) or Möbius-like bands (in the case of a single SD) depending on whether a number of vertices linked by the corresponding SD to close the orbit is even or odd respectively [26].

A convenient way of representing motions in B_R can be obtained by *unfolding* the polygon by its repeating reflections by the sides on which the trajectory reflections are performed. A frequently complicated pattern of the real trajectories takes then a simple form of parallel straight lines on such unfolded polygons.

2.2. Basic semiclassical wave functions defined on a skeleton

Consider now the stationary Schrödinger equation in the rational polygon billiard B_R

$$\left(\frac{\partial^2}{\partial x^2} + \frac{\partial^2}{\partial y^2} \right) \Psi(x, y) + \frac{2m}{\hbar^2} E \Psi(x, y) \equiv \left(\Delta + \frac{2m}{\hbar^2} E \right) \Psi(x, y) = 0 \quad (2)$$

with a ball of a mass m . For convenience, we shall put further $\hbar = 1$ and $m = 1$.

Consider also a skeleton $\mathbf{B} = \bigcup_{i=1}^n B_i$ which can be defined in the billiards, Fig. 1. Each of its bundles B_i , $i = 1, \dots, n$, contains a family of trajectories which can be locally used as new coordinates defined by:

$$\begin{aligned} x &= x_0(s_i) + d_i \cos(\alpha_i + \beta_i), \\ y &= y_0(s_i) + d_i \sin(\alpha_i + \beta_i), \end{aligned} \quad (3)$$

where according to Fig. 1, s_i is a distance of the vertex A_k from the point of the billiard side which the trajectory emerges of and d_i is a distance traveled by the billiard ball along the trajectory by the time t , *i.e.* $d_i = pt$, where p is the *classical* momentum of the ball.

On a bundle B_i , we can define the following two *basic* semiclassical wave functions (BSWF) to the Eq. (2)

$$\Psi_i^\sigma(d_i, s_i, p) = e^{\sigma i S(d_i, s_i)} \chi_i^\sigma(d_i, s_i, p), \quad i = 1, \dots, n, \quad (4)$$

where $\sigma = \pm$ is the signature of $\Psi_i^\sigma(x, y)$ and $S(d_i, s_i) = \int_{A_i}^{(x,y)} p_x dx + p_y dy = pd_i + ps_i \cos \alpha_i$ and the factor $\chi_i^\sigma(d_i, s_i, p)$ is given by the following semiclassical series for $p \rightarrow +\infty$

$$\chi_i^\sigma(d_i, s_i, p) = \sum_{m \geq 0} \frac{\chi_{i,m}^\sigma(d_i, s_i)}{p^i}. \quad (5)$$

We are looking for the energy spectrum problem of the rational polygon billiards in the form of the respective semiclassical series

$$E = \frac{1}{2} p^2 + \sum_{i \geq 0} \frac{E_i}{p^i}. \quad (6)$$

Substituting the asymptotic representations (4)–(6) to Eq. (2) (and dropping the bundle index), we get

$$\sigma 2ip \frac{\partial \chi^\sigma(d, s, p)}{\partial d} + \Delta \chi^\sigma(d, s, p) + \left(E - \frac{1}{2} p^2 \right) \chi^\sigma(d, s, p) = 0, \quad (7)$$

or

$$\begin{aligned} \frac{\partial \chi_0^\sigma(d, s)}{\partial d} &= 0, \\ \frac{\partial \chi_{k+1}^\sigma(d, s)}{\partial d} &= \frac{\sigma i}{2} \left(\Delta \chi_k^\sigma(d, s) + 2 \sum_{l=0}^k E_{k-l} \chi_l^\sigma(d, s) \right), \\ k &= 0, 1, 2, \dots, \end{aligned} \tag{8}$$

with the obvious solutions

$$\begin{aligned} \chi_0^\sigma(d, s) &\equiv \chi_0^\sigma(s) \\ \chi_{k+1}^\sigma(d, s) &= \chi_{k+1}^\sigma(s) + \frac{\sigma i}{2} \int_0^d \left(\Delta \chi_k^\sigma(a, s) + 2 \sum_{l=0}^k E_{k-l} \chi_l^\sigma(a, s) \right) da, \\ k &= 0, 1, 2, \dots \end{aligned} \tag{9}$$

Each BSWF on a bundle on which it is defined has to satisfy the following *boundary* conditions:

- if two neighbor bundles have as a piece of their boundary a common ray then the BSWFs (of the same signature) defined on these bundles have to coincide on this common ray; and
- BSWF should vanish on a boundary ray of the bundle if the ray is not common with any other bundle; and
- BSWF should vanish outside the bundle on which it is defined.

All of the above conditions ensure the continuity of a global semiclassical wave function built out of the corresponding BSWFs on the skeleton.

However, the last two demands are, in fact, the intrinsic demands of the semiclassical method since it is asymptotic. Because of that it neglects all these contributions from the exact wave functions to BSWFs which are exponentially vanishing when $p \rightarrow \infty$. Such a property has to have the exact wave functions outside the skeleton areas and, therefore, they cannot be represented there by BSWFs, *i.e.* the latter can exist only *inside* their bundles.

2.3. Global semiclassical wave functions defined on a skeleton

Let $\mathbf{B} = \bigcup_{i=1}^n B_i$ be a skeleton in B_R . We can define on the skeleton \mathbf{B} the following two continuous *global* semiclassical solutions (GSWF)

$$\Psi^{\sigma, as}(x, y) = \sum_{i=1}^n \Psi_i^\sigma(d_i(x, y), s_i(x, y), p). \tag{10}$$

It follows from the previous discussion that each $\Psi_i^\sigma(d_i(x, y), s_i(x, y), p)$, $i = 1, \dots, n$, contributes effectively to $\Psi^{\sigma,as}(x, y)$ in the corresponding bundles only.

Demanding of vanishing of $\Psi^{\sigma,as}(x, y)$ on the B_R -boundary provides us with the semiclassical solutions to the self energy problem in B_R with the help of the skeleton \mathbf{B} .

It follows from (10) that if $\Psi^{+,as}(x, y)$ is a solution to the self energy problem then its complex conjugation is also such a solution with the same energy and $\Psi^{-,as}(x, y) = (\Psi^{+,as}(x, y))^*$, *i.e.* if $\Psi^{+,as}(x, y)$ is essentially complex then the corresponding energy level is degenerated. In fact, as we will see in the next sections, such a degeneracy is typical for the GSWF's built on periodic skeletons with some rare exceptions, however.

3. Periodic skeletons in the rectangular billiards

We shall start with the simplest billiard — the rectangular one with the sides a and b . Unexpectedly, it is not as trivial as it can be thought. Simultaneously, its consideration can serve us as an archetype of similar constructions made for other billiards investigated further.

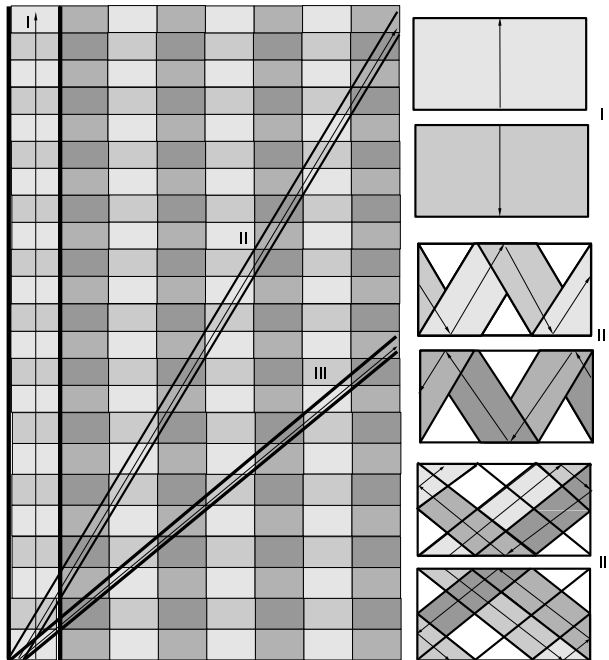


Fig. 2. Three unfolded periodic skeletons defined by the corresponding pairs of SD's. Every skeleton is the cylinder-like Lagrange surface in the phase space.

Periodic skeletons in the rectangular billiards are defined by singular diagonals linking two different vertices. The partner diagonals link the remaining two vertices by a symmetric way. Five examples of such skeletons are shown in Fig. 2 and Fig. 3 in their unfolded form (the left picture) and in their real form in the billiards (the right pictures). Each pair of SD's defining each skeleton is visible in the unfolded form of the skeletons as two parallel straight lines. Each skeleton is a stripe bounded by such two SD's. A general property of each such a stripe is that all the rectangle vertices related with the stripe lie on its boundary, *i.e.* on its two SD's. This means that none bundle of the skeletons is scattered by any rectangular vertex being totally reflected by the billiard sides into another bundle of the skeleton.

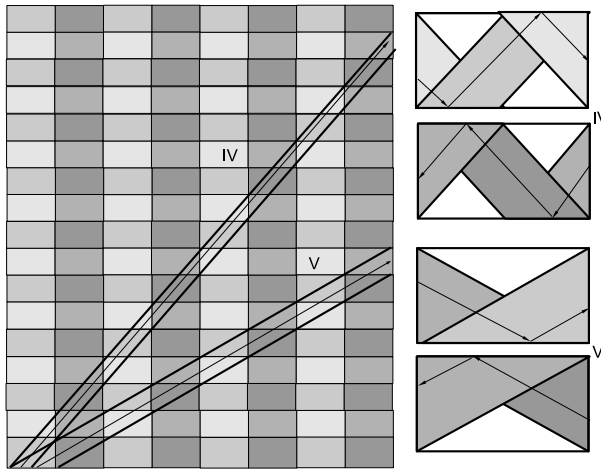


Fig. 3. Another two unfolded periodic skeletons defined by the corresponding pairs of SD's with the same cylinder-like Lagrange surfaces in the phase space.

Single periodic trajectories are shown also in each skeleton case in the figure being parallel to the SD's defining skeletons. In the billiards (the right pictures) these periodic trajectories are, of course, closed. The skeletons on the figure have forms which are typical, *i.e.* infinitely many others differ from these on the figure by a number of reflections of SD's on the rectangle sizes.

3.1. Bouncing ball skeleton and the corresponding global semiclassical wave functions

Consider the simplest periodic skeleton in the rectangle billiards numbered as *I* in Fig. 2 and shown in Fig. 4. It is defined by two SD's L_1 and L_2 linking the vertices A_1 with A_4 and A_2 with A_3 , respectively, and construct on this skeleton global semiclassical solutions with the rules mentioned in Sec. 2 and in [13]. This bouncing ball skeleton contains only two bundles B_1

and B_2 — the first one with its rays directed up and starting from the side A_1 and the second B_2 with rays directed down starting from the side A_3 . The skeleton \mathbf{B} is singular since the sides A_2 and A_4 are not covered by the bundles of the skeleton.

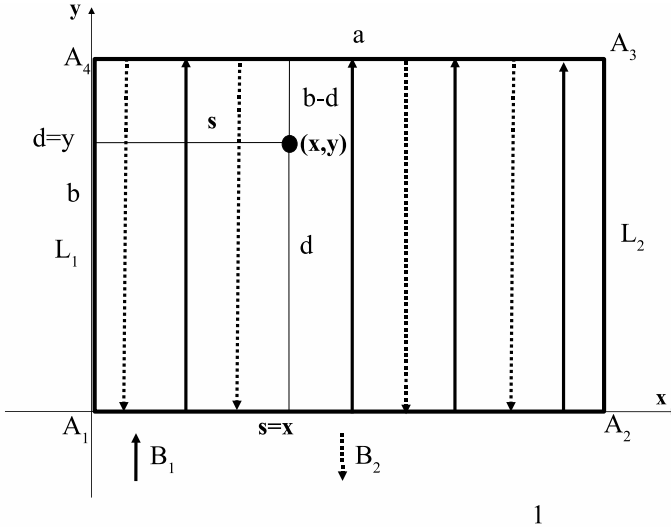


Fig. 4. The two bouncing mode bundles B_1 and B_2 of the vertical skeleton in the rectangular billiards.

The bundle rays for both the bundles B_1 and B_2 can be positioned by the same parameter s measuring a distance of a ray from the y -axis along the corresponding sides A_1 and A_3 . Therefore, for the corresponding basic semiclassical wave functions (BSWF), we have

$$\begin{aligned} \Psi_1(d, s, p) &= e^{ipd} \chi_1(d, s, p), \\ \Psi_2(b - d, s, p) &= e^{ip(b-d)} \chi_2(b - d, s, p), \\ 0 \leq d \leq b, \quad 0 < s < a. \end{aligned} \tag{11}$$

For the coefficients $\chi_k(d, s, p)$, $k = 1, 2$, it is assumed that they propagate along the rays of the bundles continuously and this their property is not influenced by reflections of the rays on the boundaries. Therefore, we have to accept also that they are periodic with respect to the d -variable with the period equal to $2b$.

For the GSWF $\Psi^{as}(x, y, p)$, we have therefore

$$\Psi^{as}(x, y, p) = \Psi_1(y, x, p) + \Psi_3(b - y, x, p) \tag{12}$$

together with the following Dirichlet boundary conditions on the sides A_1 and A_3 respectively

$$\begin{aligned}\chi_1(0, x, p) + e^{ipb}\chi_2(b, x, p) &= 0, \\ e^{ipb}\chi_1(b, x, p) + \chi_2(0, x, p) &= 0,\end{aligned}\tag{13}$$

so that in the zeroth order, we have to have

$$\chi_{1,0}(x) = e^{2ipb}\chi_{1,0}(x).\tag{14}$$

Therefore, we conclude that

$$pb = n\pi, \quad n = 1, 2, 3, \dots\tag{15}$$

Now, the corresponding boundary conditions for $\Psi_k(y, x, p)$, $k = 1, 2$ on the sides A_2 and A_4 give

$$\chi_k(y, 0, p) = \chi_k(y, a, p) \equiv 0, \quad k = 1, 3.\tag{16}$$

Therefore, in the zeroth order, we have

$$\chi_{1,0}(0) = \chi_{1,0}(a) = 0.\tag{17}$$

Now, the corresponding boundary conditions for $\Psi_k(y, x, p)$, $k = 1, 3$ on the sides A_2 and A_4 give

$$\chi_k(y, 0, p) = \chi_k(y, a, p) \equiv 0, \quad k = 1, 3.\tag{18}$$

Therefore, in the zeroth order, we have

$$\chi_{1,0}(0) = \chi_{1,0}(a) = 0.\tag{19}$$

Next, let us invoke the second of the equations (9) and the periodicity of $\chi_1(y, x, p)$ to get in the considered case for the second order term

$$\chi_{1,1}(2b, x) = \chi_{1,1}(0, x) = \chi_{1,1}(0, x) + \frac{ib}{2} \left(\frac{d^2\chi_{1,0}(x)}{dx^2} + 2E_0\chi_{1,0}(x) \right),\tag{20}$$

so that

$$\frac{d^2\chi_{1,0}(x)}{dx^2} + 2E_0\chi_{1,0}(x) = 0.\tag{21}$$

The obvious solution of the last equation satisfying the boundary conditions (16) is

$$\begin{aligned}\chi_{1,0}(x) &= A_0 \sin \left(\sqrt{2E_0}x \right), \\ \sqrt{2E_0}a &= m\pi, \quad m = 1, 2, \dots\end{aligned}\tag{22}$$

Coming back to the second of the equations (9), we can conclude that $\chi_{1,1}(y, x)$ is again independent of y .

Passing next to the third of the equations (9) and repeating arguments similar to those which led us to (20), we get the following equation for $\chi_{1,1}(x)$

$$\frac{d^2\chi_{1,1}(x)}{dx^2} + 2E_0\chi_{1,1}(x) + 2E_1\chi_{1,0}(x) = 0 \tag{23}$$

with the solution

$$\chi_{1,1}(x) = A_1 \sin(\sqrt{2E_0}x) + B_1 \cos(\sqrt{2E_0}x) + \frac{E_1 A_0 x}{\sqrt{2E_0}} \cos(\sqrt{2E_0}x) \tag{24}$$

The boundary conditions $\chi_{1,1}(0) = \chi_{1,1}(a) = 0$ enforce, however, $B_1 = E_1 = 0$.

Using again (9) and the inductive arguments, we come to the conclusion that $\chi_1(y, x, p)$ is y -independent and the coefficients of its semiclassical series have the form

$$\chi_{1,k}(x) = A_k \sin(\sqrt{2E_0}x), \quad k = 0, 1, \dots \tag{25}$$

so is the form of $\chi_1(x, p)$ itself, *i.e.*

$$\begin{aligned} \chi_1(x, p) &= A(p) \sin(\sqrt{2E_0}x) = A(p) \sin\left(m\pi \frac{x}{a}\right), \\ A(p) &= \sum_{k \geq 0} A_k p^{-k}. \end{aligned} \tag{26}$$

Clearly, similar conclusion can be obtained for $\chi_2(y, x, p)$ which by (13) and for the m th energy level is equal to

$$\chi_{2,mn}(y, x, p) = -(-1)^n \chi_{1,m}(x, p) = -(-1)^n A(p) \sin\left(m\pi \frac{x}{a}\right). \tag{27}$$

Therefore, coming back to (12), we get

$$\Psi_{mn}^{as}(x, y, p) = 2iA(p) \sin\left(n\pi \frac{y}{b}\right) \sin\left(m\pi \frac{x}{a}\right), \tag{28}$$

which appears to coincide up to an unessential constant with the known exact results for the rectangular well.

The energy E is given, however, by the *finite* semiclassical series

$$E = \frac{1}{2}p^2 + E_0 = \frac{1}{2} \left(\left(\frac{n\pi}{b}\right)^2 + \left(\frac{m\pi}{a}\right)^2 \right), \quad m, n = 1, 2, \dots \tag{29}$$

Of course, the above energy levels are all non-degenerate.

Let us note, however, that since we are working in the semiclassical limit $p \rightarrow \infty$, the real value of the approximation should be considered under the condition $\frac{1}{2}p^2 \gg E_0$, so that the numbers m, n in (29) should satisfy

$$m \ll \frac{a}{b}n. \quad (30)$$

The above condition is essentially the one of Bogomolny *et al.* [19] for validity of their asymptotic results on the existence of the superscar states.

However, in the particular case of the skeleton considered the superscar states it generates appear to coincide with the exact ones. A reason for that is that its two bundles if closed cover each completely the rectangular billiards. It is not the case for other periodic skeletons which exist in this billiards and which will be considered next below.

3.2. Exact solutions of the Schrödinger equation on the Lagrange surfaces and their relations with GSWF's in periodic skeletons

Let us now note that the skeleton considered is just the projection of the Lagrange surface corresponding to it and having the form of the cylinder-like band with the radius $\frac{b}{\pi}$ and the side a so that if unfolded on the plane this surface is again a rectangle with the sides a and $2b$.

Let us treat this cylinder-like Lagrange surface as a billiard table and consider the Schrödinger equation (2) on it and its corresponding energy spectrum problem. Let us call the billiards the Lagrange surface billiards (LSB) corresponding to the bouncing ball skeleton. Let x, y , $0 \leq x \leq a$, $0 \leq y \leq 2b$, be the coordinates on the unfolded cylinder and consider solutions to the energy spectrum problem of the forms $\Psi^\pm(x, y, p) = e^{\pm ipy} \chi(x)$ satisfying the conditions to be *periodic* on the cylinder and *vanishing* on its boundaries. The obvious two independent *exact* solutions to the problem are the following:

$$\begin{aligned} \Psi_{mn}^\pm(x, y, p_n) &= e^{\pm ip_n y} \sin\left(m\pi \frac{x}{a}\right), \\ p_n &= \frac{n\pi}{b}, \\ E_{mn} &= \frac{1}{2}p_n^2 + \frac{m^2\pi^2}{a^2}, \\ m, n &= 1, 2, \dots \end{aligned} \quad (31)$$

i.e. the above energy spectrum coincides exactly with (29).

It is not difficult to see that the GSWF (28) can be now obtained in the following way

$$\Psi_{mn}^{as}(x, y, p_n) = A(p_n) (\Psi_{mn}^+(x, y, p_n) - \Psi_{mn}^+(x, 2b - y, p_n)) \quad (32)$$

i.e. as an appropriate linear combinations of the *exact* solutions (31) taken at the points of the cylinder which are projected on the point (x, y) of the rectangular billiards. Coefficients of the respective linear combination have to be taken in such a way to ensure the vanishing of the combination on the respective parts of the billiard boundary.

We will convince ourselves below that this is the universal property of the superscar states suggested, in fact, as the way of their constructions by Bogomolny *et al.* [19, 20].

In the next section, we will show also that LSB's which correspond to each periodic orbit skeleton in the RPB's have shapes of the cylinder-like or the Möbius-like bands on which the exact solutions to the Schrödinger equation exist.

We will also convince ourselves that the rectangular billiards and more generally the RPB's create opportunity for the stationary states of the corresponding LSB's to manifest themselves in the form of the semiclassical wave functions defined on the periodic skeletons. We shall discuss wider this relation later.

3.3. Other periodic skeletons in the rectangular billiards

Consider now other periodic skeletons in the rectangle. The simplest such a case is the fifth one in Fig. 2 and shown in Fig. 5. It is defined by two SD's which are the two rectangle diagonals. In this case, there are four bundles B_k , $k = 1, \dots, 4$, in the corresponding skeleton in the forms of triangles: $B_1 = \triangle A_1A_2A_3$, $B_2 = \triangle A_2A_3A_4, \dots$. There are always two rays (of the four of them) belonging to two different bundles which can meet at each point of the rectangle if this point does not lie on SD's.

We have to note also that the skeleton associated with this in Fig. 5 differs from it by the opposite directions of rays, *i.e.* possible energy levels we get for these skeletons must be degenerated.

The GSWF corresponding to the case looks as follows in different domains of the rectangles:

$$\Psi^{+,as}(x, y) = \begin{cases} e^{ipd_1+ips_1 \cos \alpha} \chi_1(d_1, s_1, p) + e^{ipd'_4+ips'_4 \sin \alpha} \chi_4(d'_4, s'_4, p) & (x, y) \in D_1 \\ e^{ipd'_1+ips'_1 \cos \alpha} \chi_1(d'_1, s'_1, p) + e^{ipd_2+ips_2 \sin \alpha} \chi_2(d_2, s_2, p) & (x, y) \in D_2 \\ e^{ipd_3+ips_3 \cos \alpha} \chi_3(d_3, s_3, p) + e^{ipd'_2+ips'_2 \sin \alpha} \chi_2(d'_2, s'_2, p) & (x, y) \in D_3 \\ e^{ipd'_3+ips'_3 \cos \alpha} \chi_3(d'_3, s'_3, p) + e^{ipd_4+ips_4 \sin \alpha} \chi_4(d_4, s_4, p) & (x, y) \in D_4 \\ \tan \alpha = \frac{b}{a} & \end{cases} \quad (33)$$

where the variables s_k, s'_k are measured from the left ends of the corresponding sides A_k , $k = 1, \dots, 4$.

The Dirichlet boundary conditions on the respective sides of the rectangle are therefore:

$$\begin{aligned}
 \chi_1(0, s, p) + e^{ipb \sin \alpha} \chi_4\left(\frac{s}{\cos \alpha}, b - s \tan \alpha, p\right) &= 0, \\
 e^{ipa \cos \alpha} \chi_1\left(\frac{a-s}{\cos \alpha}, s, p\right) + \chi_2(0, (a-s) \tan \alpha, p) &= 0, \\
 \chi_3(0, s, p) + e^{ipb \sin \alpha} \chi_2\left(\frac{s}{\cos \alpha}, (a-s) \tan \alpha, p\right) &= 0, \\
 e^{ipa \cos \alpha} \chi_3\left(\frac{a-s}{\cos \alpha}, s, p\right) + \chi_4(0, b - s \tan \alpha, p) &= 0, \\
 0 < s < a. & \tag{34}
 \end{aligned}$$

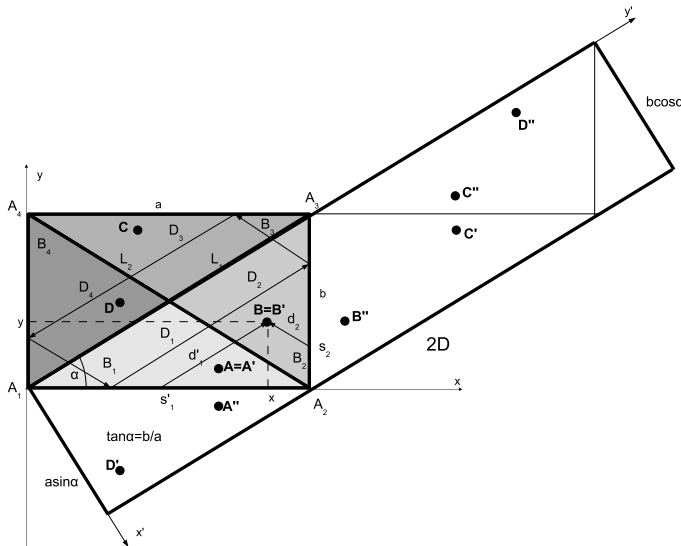


Fig. 5. The periodic skeleton defined by the corresponding pair L_1 and L_2 of SD's and its unfolded Lagrange surface.

One can easily find from (34) that

$$\chi_1(0, s, p) = e^{2ip(b \sin \alpha + a \cos \alpha)} \chi_1\left(\frac{2a}{\cos \alpha}, s, p\right) \tag{35}$$

or

$$e^{2ip(b \sin \alpha + a \cos \alpha)} = 1 \tag{36}$$

because $\chi_1(d, s, p)$ is periodic with the period $\frac{2a}{\cos \alpha} = 2(b \sin \alpha + a \cos \alpha) = 2D$, where D is the length of the rectangle diagonal.

Therefore, we get the following quantization condition for the momentum p

$$pD = n\pi, \quad n = 1, 2, \dots \tag{37}$$

Now, we have to note that none of the four boundary rays coinciding with one of the diagonals is common for any pair of the bundles considered since the rays seemingly pretending to have this property are, in fact, *opposite*. Therefore, BSWFs defined in the bundles have to vanish on the respective diagonals of the rectangle, so that we have to have

$$\begin{aligned} \chi_k(d, 0, p) &= 0, & k &= 1, \dots, 4, \\ 0 &\leq d \leq D. \end{aligned} \tag{38}$$

But then from (34), we get also

$$\chi_1(0, a, p) = \chi_2(0, b, p) = \chi_3(0, a, p) = \chi_4(0, b, p) = 0. \tag{39}$$

Further, using the propagation formula (9) for $\chi_{1,1}(2D, s) = \chi_{1,1}(0, s)$, we get

$$\chi''_{1,0}(s) + 2E_0 \sin^2 \alpha \chi_{1,0}(s) = 0 \tag{40}$$

which, with the conditions (38)–(39) for $\chi_1(d, s, p)$, gives

$$\chi_{1,0}(s) = A_0 \sin \left(\sqrt{2E_0} \sin \alpha s \right), \tag{41}$$

where E_0 defines the second term of the semiclassical energy expansion with the condition

$$E_0 = \frac{1}{2} \frac{m^2 \pi^2}{a^2 \sin^2 \alpha}, \quad m = 1, 2, 3, \dots \tag{42}$$

Next, repeating the procedure for the bouncing mode skeleton to the remaining terms $\chi_{1,k}(2D, s) = \chi_{1,k}(0, s)$, $k = 1, 2, 3, \dots$, we get for them

$$\chi_{1,k}(s) = A_k \sin \left(\sqrt{2E_0} \sin \alpha s \right), \tag{43}$$

so that

$$\begin{aligned} \chi_1(d, s, p) &= A(p) \sin \left(\sqrt{2E_0} \sin \alpha s \right), \\ A(p) &= \sum_{k \geq 0} A_k p^{-k}. \end{aligned} \tag{44}$$

Therefore, using (34), the final form of the GSWF $\Psi^{as}(x, y)$ can be written as follows:

$$\Psi_{mn}^{+,as}(x, y) = \begin{cases} \begin{aligned} &e^{ip_n(x \cos \alpha + y \sin \alpha)} \sin\left(m\pi \frac{1}{a}(x - y \cot \alpha)\right) \\ &-e^{ip_n(x \cos \alpha - y \sin \alpha)} \sin\left(m\pi \frac{1}{a}(x + y \cot \alpha)\right) \end{aligned} & (x, y) \in D_1 \\ \begin{aligned} &e^{ip_n(x \cos \alpha + y \sin \alpha)} \sin\left(m\pi \frac{1}{a}(x - y \cot \alpha)\right) \\ &+e^{ip_n(-x \cos \alpha + y \sin \alpha + 2a \cos \alpha)} \sin\left(m\pi \frac{1}{a}(x + y \cot \alpha)\right) \end{aligned} & (x, y) \in D_2 \\ \begin{aligned} &-e^{ip_n(-x \cos \alpha - y \sin \alpha)} \sin\left(m\pi \frac{1}{a}(x - y \cot \alpha)\right) \\ &+e^{ip_n(-x \cos \alpha + y \sin \alpha + 2a \cos \alpha)} \sin\left(m\pi \frac{1}{a}(x + y \cot \alpha)\right) \end{aligned} & (x, y) \in D_3 \\ \begin{aligned} &-e^{ip_n(-x \cos \alpha - y \sin \alpha)} \sin\left(m\pi \frac{1}{a}(x - y \cot \alpha)\right) \\ &-e^{ip_n(x \cos \alpha - y \sin \alpha)} \sin\left(m\pi \frac{1}{a}(x + y \cot \alpha)\right) \end{aligned} & (x, y) \in D_4 \end{cases}, \tag{45}$$

while the energy spectrum is

$$E = \frac{1}{2}p^2 + E_0 = \frac{\pi^2}{2} \left(\frac{n^2}{D^2} + \frac{m^2 D^2}{a^2 b^2} \right), \quad m, n = 1, 2, 3, \dots \tag{46}$$

By their construction, the solutions (45) are all *singular* in the rectangle — their derivatives are discontinuous on the rectangle diagonals.

Moreover, the corresponding energy spectrum differs this time from the exact one of the bouncing ball skeleton.

However, a property common with the bouncing ball skeleton is the form of the Lagrange surface corresponding to the skeleton of Fig. 5 which, again, is a cylinder-like band with the radius equal to $\frac{D}{\pi}$ and with the height equal to $a \sin \alpha = b \cos \alpha$. Unfolding this Lagrange surface into rectangle $D \times a \sin \alpha$ (see Fig. 5) and considering it as a billiard table, we get directly from (31) the following *exact* results for the quantized ball energy in the billiard and its wave functions:

$$\begin{aligned} \Psi_{mn}^\pm(x', y', p_n) &= e^{\pm ip_n y'} \sin\left(m\pi \frac{x'}{a \sin \alpha}\right), \\ p_n &= \frac{n\pi}{D}, \\ E_{mn} &= \frac{1}{2}p_n^2 + \frac{m^2 \pi^2}{a^2 \sin^2 \alpha}, \\ m, n &= 1, 2, \dots, \end{aligned} \tag{47}$$

where x' is a coordinate along the side $a \sin \alpha$ and y' — along the side $2D$, see Fig. 5.

Again, we can rewrite the GSWF's (45) by the linear combinations of the *exact* solutions (47) using Fig. 5, where the points A, B, C, D are mapped into the following pairs of the Lagrange surface points $(A', A''), (B', B''), (C', C''), (D', D'')$, respectively. Namely, according to Fig. 5, we get:

$$\Psi_{mn}^{+,as}(x, y, p_n) = \begin{cases} \Psi_{mn}^+(x'_{A'}, y'_{A'}, p_n) - \Psi_{mn}^+(x'_{A''}, y'_{A''}, p_n) & (x_A, y_A) \in D_1 \\ \Psi_{mn}^+(x'_{B'}, y'_{B'}, p_n) - \Psi_{mn}^+(x'_{B''}, y'_{B''}, p_n) & (x_B, y_B) \in D_2 \\ -\Psi_{mn}^+(x'_{C'}, y'_{C'}, p_n) + \Psi_{mn}^+(x'_{C''}, y'_{C''}, p_n) & (x_C, y_C) \in D_3 \\ -\Psi_{mn}^+(x'_{D'}, y'_{D'}, p_n) + \Psi_{mn}^+(x'_{D''}, y'_{D''}, p_n) & (x_D, y_D) \in D_4 \end{cases}, \tag{48}$$

where (x', y') are related with (x, y) by the rotation by the angle $\alpha - \frac{1}{2}\pi$.

Therefore, we get again a picture of the GSWF (45) as the semiclassical realization of the exact solutions existing on the Lagrange surface corresponding to the skeleton of Fig. 5 and playing, in this way, a role of resonant modes in the rectangular billiards in the high energy limit.

Since the solutions (45)–(46) are *allowed* semiclassical solutions to the rectangle billiards eigenvalue problem it is of great importance whether one can detect in these limits such resonant modes in the respective rectangular cavity. In fact, such modes have been detected experimentally by Bogomolny *et al.* [20] for the rectangle cavity with a *barrier* inside. This case of the billiards will be discussed in the next sections.

If, however, such modes can be detected in the rectangle cavity then one can expect the corresponding GSWF's to have the forms of standing waves rather than of the running ones as in (45) or (48). We can get such forms of GSWF's noticing that the spectrum (46) is obviously degenerate since in the case considered the solutions (48) are complex. Therefore, their complex conjugations form the solutions $\Psi_{mn}^{-,as}(x, y, p_n)$ with the same spectrum. We can use them, therefore, to construct by superpositions the standing GSWF's corresponding to the energy spectrum (46).

Due to its asymptotic sense, the GSWF's (45) should be tested in the high energy limit when $\frac{1}{2}p^2 \gg 2E_0$, *i.e.* according to (47) when

$$m \ll \frac{ab}{D^2}n. \tag{49}$$

The above results can be generalized to arbitrary periodic skeletons in the rectangular billiards some of which are shown in Fig. 2 and Fig. 3. We only sketch such a generalization.

This can be done by noticing that an arbitrary periodic SD is defined by arbitrary two coprime numbers $\{r, q\}$, so that an SD in a rectangle with the sides a and b shown in Fig. 5 starting from the vertex $(0, 0)$ and being inclined by an angle α to the x -axis, it is defined by such two numbers as follows

$$\tan \alpha = \frac{rb}{qa}. \tag{50}$$

The above fact is a direct consequence of the unfolded forms of periodic trajectories shown in Fig. 2 and Fig. 3 if one realizes that each of them has to finish on another vertex of the rectangle. It follows also that the set of all SD is countable but dense among all trajectories in the rectangle.

Pairs $\{r, q\}$ can appear in the following combinations $\{e, o\}$, $\{o, o\}$ and $\{o, e\}$, where e stands for “even” and o — for “odd”. The respective SD’s defined by these combinations finish their runs in the vertices $(a, 0)$, (a, b) and $(0, b)$, correspondingly.

An SD defined by a pair $\{r, q\}$ bounces $r - 1$ -times from each horizontal side of the rectangle and $q - 1$ -times — from each of the vertical ones. If D denotes its global length measured from its starting vertex $(0, 0)$ to one of its final ones just enumerated, then $D = rb \sin \alpha + qa \cos \alpha = \sqrt{(qa)^2 + (rb)^2}$.

If an SD is chosen, *i.e.* $\{r, q\}$ are fixed, and it ends at one of the vertices just enumerated then the second SD which has to accompany the chosen one to build the skeleton starts and ends at the remaining two of these vertices. Note that a number of bundles in such a skeleton is then equal to $2r + 2q$, while their widths are equal to $w = \frac{a}{r} \sin \alpha = \frac{b}{q} \cos \alpha$. Each bundle is crossed by another bundle only once but it is crossed by such bundles along its whole length, so that each point of the billiards lies in a crossing area of some *two* bundles excluding points which lie on the boundaries of the bundles.

Therefore, in the phase space, the corresponding Lagrange surface is again a cylinder-like band with the radius $\frac{D}{\pi}$ and with the width w . The quantization of the unfolded LSB in the form of the rectangular billiards $D \times w$ leads us immediately to the following obvious result:

$$\begin{aligned} \Psi_{mn}^{\pm}(x', y', p_n) &= e^{\pm i p_n y'} \sin \left(m \pi \frac{x'}{w} \right), \\ p_n &= \frac{n \pi}{D}, \\ E_{mn} &= \frac{1}{2} p_n^2 + \frac{m^2 \pi^2}{w^2}, \\ m, n &= 1, 2, \dots, \end{aligned} \tag{51}$$

where x' is the coordinate along the side w and y' — along the side $2D$ of the unfolded Lagrange surface.

The GSWF’s can be constructed similarly to the previous cases with the help of the solutions (47) as their proper linear combinations in the respective crossing areas of the bundles of the skeleton using the fact that each point of the billiard is always mapped into two points of the Lagrange surface. Again, the GSWF’s can be considered as the resonant manifestation in the rectangular billiards of the exact solutions (51) on the Lagrange surface in the high energy limit for which

$$m \ll \frac{w}{D} n. \tag{52}$$

The GSWF's constructed in this way are all singular having discontinuous derivatives on the lines separating two neighboring bundles. The lines are just the bundles boundaries on which the BSWFs defined in these bundles have to vanish.

4. Periodic skeletons in pseudointegrable billiards and their quantization — broken rectangles

By a broken rectangle we mean the one which can be decomposed into a finite set of disjoint rectangles, see Fig. 6. If reintegrated, it shows some number of rectangular bays and peninsulas.

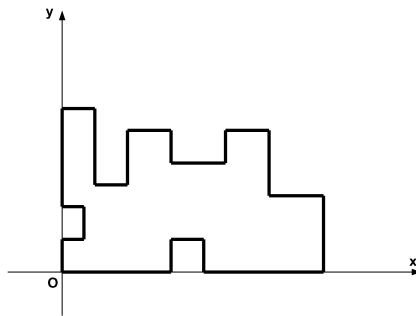


Fig. 6. An “arbitrary” broken rectangular billiard.

In fact, the broken rectangles can serve as archetypes of pseudointegrable systems with an arbitrary genus. Since, however, we are interested in considering some special SWF's configurations related to classical periodic trajectories, we shall limit ourselves to rather simple forms of the broken rectangles. The simplest one with a single peninsula (the L-shaped pseu-

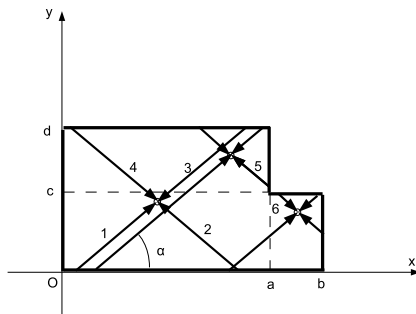


Fig. 7. A single bay rectangular billiard with a “generic” global singular skeleton composed of six bundles. Its reduced form contains four global but singular compound bundles which form in the phase space the closed Lagrange surface of genus 2.

dointegrable billiards in terms of Kudrolli and Sridhar [21]) is shown in Fig. 7 and also in Fig. 8 and Fig. 9 with several skeleton configurations related to some SD.

The skeleton in Fig. 7 is shown only as an example the corresponding Lagrange surface of which is two dimensional with genus equal to 2.

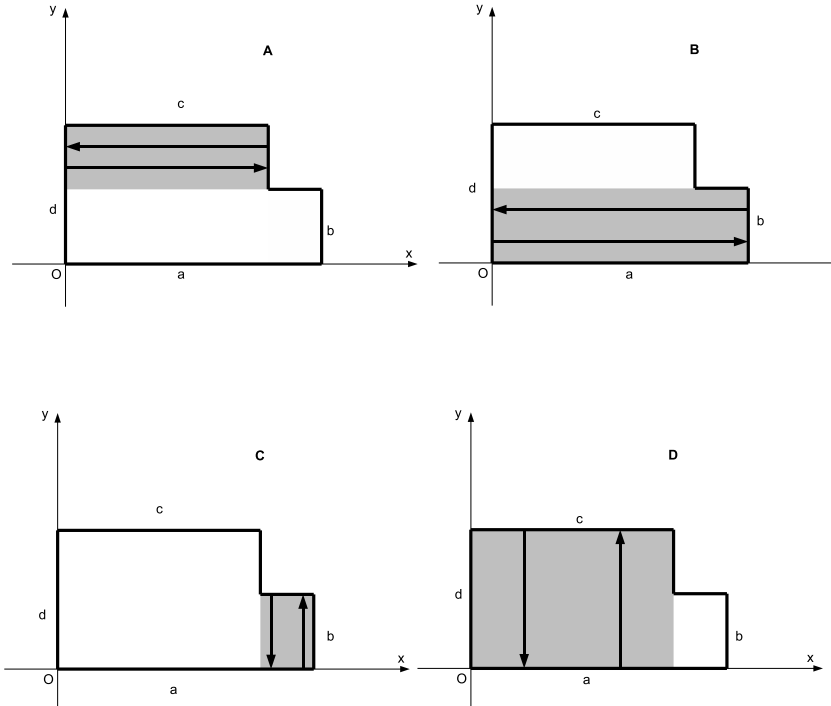


Fig. 8. A single bay rectangular billiard with periodic skeletons — the singular bouncing ball cases. Every skeleton forms the cylinder-like Lagrange surface in the phase space.

However, we are rather interested in the periodic skeletons in the considered broken rectangular billiards. Examples of them correspond to all the skeletons shown in Fig. 8 and Fig. 9.

The skeletons of Fig. 8 define GSWF's which are identical with the ones of the formulae (28) and (29) with respective substitutions. These modes were observed experimentally by Kudrolli and Sridhar [21].

Even more spectacular are skeletons built by periodic orbits different than the bouncing ball ones shown in Fig. 9. These are just the skeletons which provide us with the singular SWF's with properties described by Bogomolny and Schmit [19] as supercars and was observed also experimentally by Kudrolli and Sridhar [21].

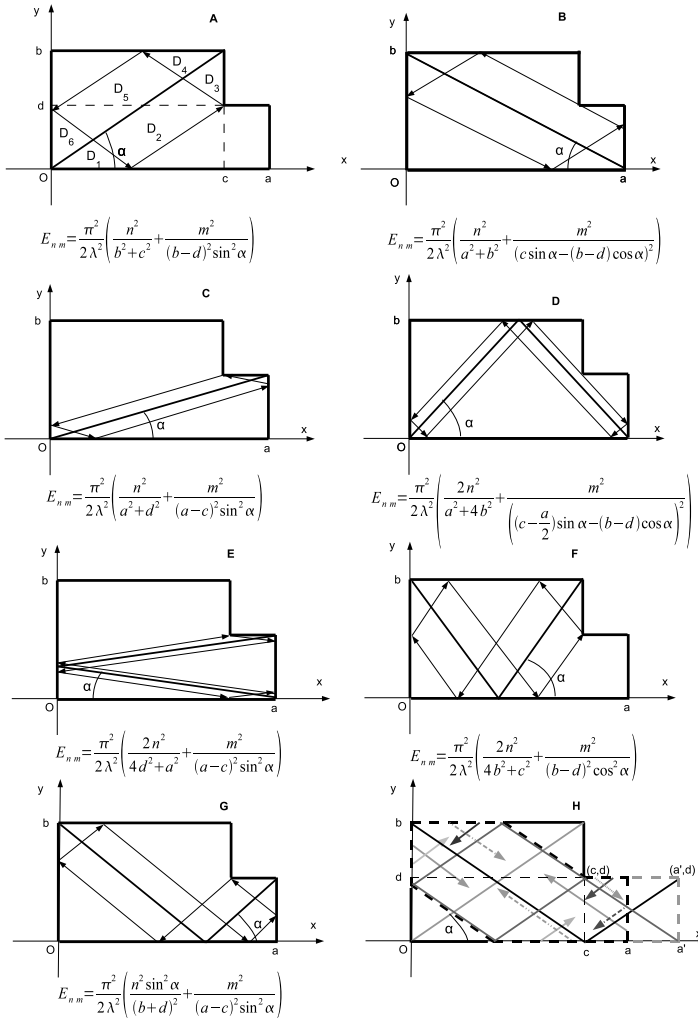


Fig. 9. A single bay rectangular billiard with singular skeletons built on the shortest periodic trajectories (black continuous rays) different than the bouncing ball ones with the energy spectra of the respective GSWF's ((A)–(G)). Note that $n, m = 1, 2, \dots$, for every spectrum. Arrows on these figures show the second periodic orbits being the second SD of Bogomolny and Schmit [19] for the corresponding skeletons. The skeletons form the cylinder-like Lagrange surfaces in the phase space each. All the spectra shown are exact on the respective Lagrange surfaces. In (H) the skeleton complementing the one of (A) is shown. It contains ten bundles. It occupies the area bounded by black dashed contour. Its Lagrange surface is a torus with three holes in its surface (see Fig. 11).

The GSWF's corresponding to the broken rectangle billiards shown in Fig. 10 (upper figures) were observed by Bogomolny *et al.* [20]. In fact, the authors mentioned the limit of the billiards considered when $d - c \rightarrow 0$ (lower figures). They studied experimentally the high frequency modes in a microwave cavity [20] confirming the existence of the superscar modes predicted earlier by Bogomolny and Schmit [19].

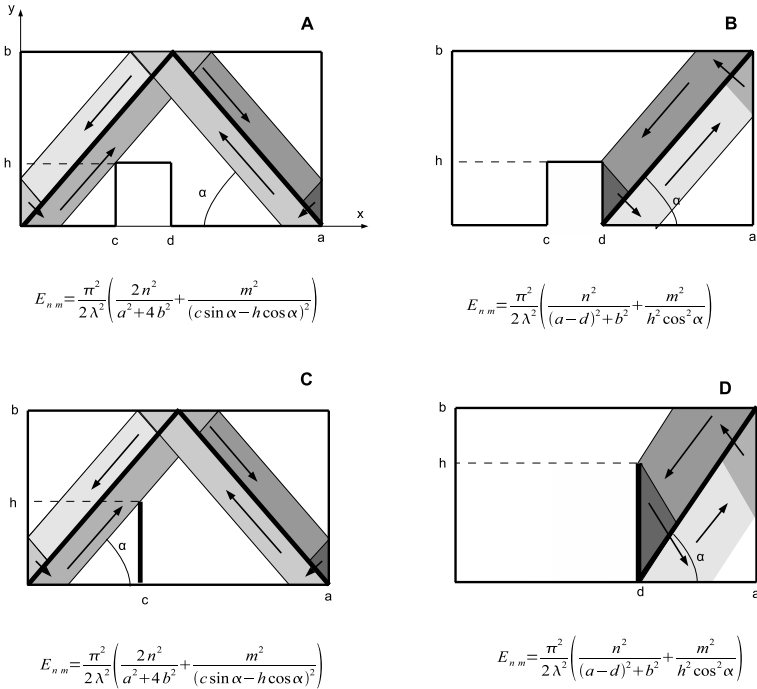


Fig.10. Broken rectangular billiards with barriers and with possible superscar skeletons and with the energy spectra corresponding to the respective GSWF's. In all the above formulae, $n, m = 1, 2, \dots$. The corresponding Lagrange surfaces in the phase space are cylinder-like.

For a completeness, we shall give below the two linearly independent GSWF's for the skeleton A of Fig. 9 together with their degenerate energy spectrum.

$$\begin{aligned}
 \Psi_{1,2,mn}^{as}(x, y) = & \\
 & \left\{ \begin{aligned}
 & \sin\left(\frac{m\pi}{c-d\cot\alpha}(x-y\cot\alpha)\right) \times \begin{cases} \sin\left(\frac{n\pi}{D}(x\cos\alpha+y\sin\alpha)\right) \\ \pm \cos\left(\frac{n\pi}{D}(x\cos\alpha+y\sin\alpha)\right) \end{cases} \\
 & - \sin\left(\frac{m\pi}{c-d\cot\alpha}(x+y\cot\alpha)\right) \times \begin{cases} \sin\left(\frac{n\pi}{D}(x\cos\alpha-y\sin\alpha)\right) \\ \cos\left(\frac{n\pi}{D}(x\cos\alpha-y\sin\alpha)\right) \end{cases} \\
 & \text{for } (x, y) \in D_1, D_6 \\
 & \sin\left(\frac{m\pi}{c-d\cot\alpha}(x-y\cot\alpha)\right) \times \begin{cases} \sin\left(\frac{n\pi}{D}(x\cos\alpha+y\sin\alpha)\right) \\ \pm \cos\left(\frac{n\pi}{D}(x\cos\alpha+y\sin\alpha)\right) \end{cases} \\
 & \text{for } (x, y) \in D_2, D_5,
 \end{aligned} \right. , \\
 \Psi_{1,2,mn}^{as}(x, y) = & \\
 & \left\{ \begin{aligned}
 & \sin\left(\frac{m\pi}{c-d\cot\alpha}(x-y\cot\alpha)\right) \times \begin{cases} \sin\left(\frac{n\pi}{D}(x\cos\alpha+y\sin\alpha)\right) \\ \pm \cos\left(\frac{n\pi}{D}(x\cos\alpha+y\sin\alpha)\right) \end{cases} \\
 & - \sin\left(\frac{m\pi}{c-d\cot\alpha}(x+y\cot\alpha)\right) \times \begin{cases} \sin\left(\frac{n\pi}{D}(x\cos\alpha-y\sin\alpha-2c\cos\alpha)\right) \\ - \cos\left(\frac{n\pi}{D}(x\cos\alpha-y\sin\alpha-2c\cos\alpha)\right) \end{cases} \\
 & \text{for } (x, y) \in D_3, D_4,
 \end{aligned} \right. , \\
 \tan\alpha = & \frac{b}{c}, \\
 pD = & n\pi, \\
 E_0 = & \frac{m^2\pi^2}{2(c\sin\alpha-d\cos\alpha)^2}, \\
 E_{mn} = & \frac{1}{2}p^2 + E_0 = \frac{\pi^2}{2} \left(\frac{n^2}{D^2} + \frac{m^2}{(c\sin\alpha-d\cos\alpha)^2} \right), \quad m, n = 1, 2, 3, \dots,
 \end{aligned} \tag{53}$$

where $D = \sqrt{b^2 + c^2}$ is the length of the diagonal shown in Fig. 9 (A).

4.1. Skeletons complementing the periodic ones in the broken rectangular billiards

It is easy to note that in the broken rectangle billiards for any periodic skeleton which is not global, there is always a closed set of trajectories accompanied it but which do not belong to it. Namely, these are trajectories which are parallel to the trajectories of the skeleton. By its closeness, these trajectories can be also collected into a set of skeletons. These skeletons will be called complementing the skeleton considered. In Fig. 9 (H), it is shown the skeleton complementing the one of Fig. 13 (A). However, since it is defined completely by the skeleton of Fig. 9 (A), it cannot have a chance to satisfy *exactly* all conditions demanded for GSWF which we could try to define on it. Nevertheless, it could be possible if, by a chance, the billiards considered would have the form suggested in the Fig. 9 (H) (by the dashed grey contour). Its Lagrange surface is a torus with three holes in its surface (see Fig. 11).

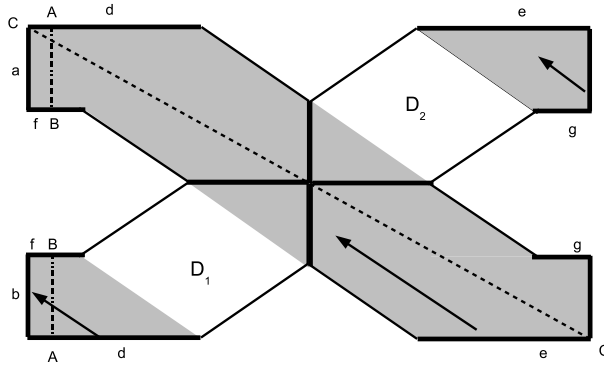


Fig. 11. The unfolded skeleton of Fig. 9 (H) complementing the one of Fig. 9 (A). Its corresponding Lagrange surface is a torus with three holes in it on which the skeleton develops a closed band leaving empty the surface area D_1 , D_2 between the holes.

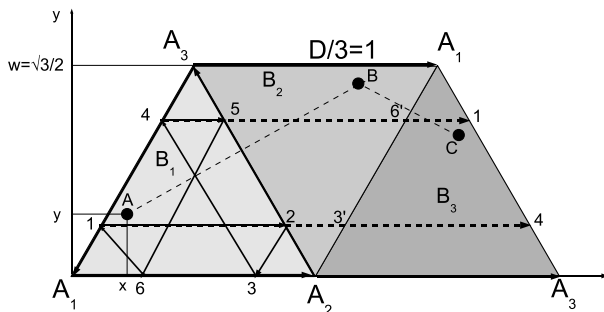


Fig. 12. The unfolded periodic skeleton in the equilateral triangle $A_1A_2A_3$ defined by the periodic orbit $A_1A_2A_3A_1$ and forming the Möbius-like band in the phase space. The skeleton contains three bundles B_1 , B_2 , B_3 with their rays parallel to the sides A_1A_2 , A_3A_1 , A_3A_2 , respectively.

In the next section, the complementing skeletons will be detected in other billiards accompanying other periodic skeletons.

5. Periodic skeletons in the triangle and the pentagon billiards

In this and in the next section, we will made a short review of the billiards systems which have been widely considered [8, 10, 20, 27, 28] both theoretically and experimentally having mainly in mind their periodic skeleton description.

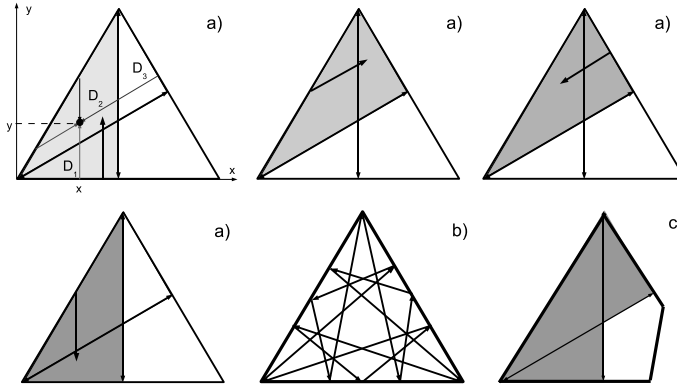


Fig. 13. Skeletons in the equilateral triangles: (a) defined by periodic orbits with a cylinder-like Langrange surface, (b) with longer periodic orbits, (c) in the amputated corner triangle. The latter can be neither integrable nor pseudointegrable.

5.1. The equilateral triangle billiards

These billiards whose dynamics is integrable have been considered in past very often [8, 17]. The simplest periodic orbits and the corresponding skeletons are shown in Fig. 12 and Fig. 13.

The periodic skeleton of Fig. 12 is defined by the SD composed of the three sides of the triangle so that the period of the orbit is equal to three. The skeleton contains only three bundles covering the whole triangle each. Therefore, to get GSWF it is enough to superpose in each point of the triangle only three BSWF defined on the bundles.

It is obvious also that on the skeleton shown in Fig. 12, one can build two linear independent GSWF's with the opposite signatures and having the same energy spectrum, *i.e.* the corresponding energy spectrum is degenerate.

Taking, therefore, two independent superpositions of these GSWF's, we get the following semiclassical solutions for the case

$$\begin{aligned}
 \Psi_{mn}^{(1)}(x, y) = & \sin\left(\frac{2}{3}m\pi x\right) \sin\left(\frac{2}{\sqrt{3}}n\pi y\right) \\
 & - \sin\left[\frac{1}{3}m\pi(x + \sqrt{3}y)\right] \sin\left[n\pi\left(x - \frac{y}{\sqrt{3}}\right)\right] \\
 & + \sin\left[\frac{1}{3}m\pi(x - \sqrt{3}y)\right] \sin\left[n\pi\left(x + \frac{y}{\sqrt{3}}\right)\right] \quad (54)
 \end{aligned}$$

and

$$\Psi_{mn}^{(2)}(x, y) = \cos\left(\frac{2}{3}m\pi x\right) \sin\left(\frac{2}{\sqrt{3}}n\pi y\right)$$

$$\begin{aligned}
& + \cos \left[\frac{1}{3} m \pi (x + \sqrt{3} y) \right] \sin \left[n \pi \left(x - \frac{y}{\sqrt{3}} \right) \right] \\
& - \cos \left[\frac{1}{3} m \pi (x - \sqrt{3} y) \right] \sin \left[n \pi \left(x + \frac{y}{\sqrt{3}} \right) \right]
\end{aligned} \tag{55}$$

with the energy spectrum

$$\begin{aligned}
E_{mn} &= \frac{2\pi^2}{9} (m^2 + 3n^2) \\
& m, n = 1, 2, \dots
\end{aligned} \tag{56}$$

for both the solutions, where m, n are even or odd simultaneously.

By their asymptotic origins, the superscar solutions (54)–(56) should be considered for $n \ll \frac{m}{\sqrt{3}}$.

However, similarly to the bouncing ball skeleton in the rectangular billiards, the above solutions and their common energy spectra are exact since the bundles of the skeleton cover the billiards totally.

In the considered case of the skeleton, the LSB corresponding to it is Möbius-like band shown in Fig. 12 with the following two linear independent *exact* solutions in such a billiard

$$\begin{aligned}
\Psi_{mn}^{\pm}(x, y) &= e^{\pm i p_m x} \sin \left(n \pi \frac{2y}{\sqrt{3}} \right) \\
3p_m &= 2m\pi, \quad m = 1, 2, \dots
\end{aligned} \tag{57}$$

and with the energy spectrum identical with (56).

Note that the x -variable in (57) is local, *i.e.* it should be continued along the dashed arrows when achieving the sides $A_1 A_3$ of the unfolded skeleton of Fig. 12. Having this in mind, the two independent semiclassical solutions in the equilateral triangle corresponding to the skeleton of Fig. 12 can be written as

$$\Psi_{mn}^{\pm, as}(x_A, y_A) = \Psi_{mn}^{\pm}(x_A, y_A) - \Psi_{mn}^{\pm}(x_B, y_B) + \Psi_{mn}^{\pm}(x_C, y_C), \tag{58}$$

where the coordinates (x_B, y_B) and (x_C, y_C) should be taken according to Fig. 12.

Once again, we see that the superscar solutions are the resonant reflections of the exact states existing in the corresponding LSB's.

In the case of the periodic skeleton of Fig. 13 (a) defined by the periodic orbit of the length $\sqrt{3}$ (the double height of the triangle), there are four bundles of the skeletons. Therefore, the two linearly independent GSWF are defined locally in the domains D_k , $k = 1, 2, 3$, of Fig. 13 (a) being, however, continuous in $D_1 \cup D_2 \cup D_3$. They are the following:

$$\Psi_{1,2;mn}^{as}(x, y) = \begin{cases} \sin(2n\pi x) \times \begin{cases} \sin\left(2m\pi\frac{x}{\sqrt{3}}\right) \\ \cos\left(2m\pi\frac{x}{\sqrt{3}}\right) \end{cases} & (x, y) \in D_1 \\ \sin(2n\pi x) \times \begin{cases} \sin\left(2m\pi\frac{x}{\sqrt{3}}\right) \\ \cos\left(2m\pi\frac{x}{\sqrt{3}}\right) \end{cases} - & \\ \sin[n\pi(x + \sqrt{3}y)] \times \begin{cases} \sin\left[m\pi\left(x + \frac{y}{\sqrt{3}}\right)\right] \\ \cos\left[m\pi\left(x + \frac{y}{\sqrt{3}}\right)\right] \end{cases} & (x, y) \in D_2 \\ -\sin[n\pi(x + \sqrt{3}y)] \times \begin{cases} \sin\left[m\pi\left(x + \frac{y}{\sqrt{3}}\right)\right] \\ \cos\left[m\pi\left(x + \frac{y}{\sqrt{3}}\right)\right] \end{cases} & (x, y) \in D_3 \end{cases} \quad (59)$$

with the energy spectrum

$$E_{mn} = \frac{2\pi^2}{3} (m^2 + 3n^2) , \quad n \ll \frac{m}{\sqrt{3}} , \quad m, n = 1, 2, \dots \quad (60)$$

Of course, $\Psi_{1,2;mn}^{as}(x, y) \equiv 0$ if $(x, y) \notin D_1 \cup D_2 \cup D_3$.

While the above $\Psi_{mn}^{as}(x, y)$ satisfies the Schrödinger equation, its derivatives are not continuous on the boundaries separating the domains D_k , $k = 1, 2, 3$. This is why it is only semiclassical approximation to the exact solutions given earlier.

One could, of course, repeat the previous arguments and rewrite the GSWF's by the exact solutions on the corresponding LSB on which the energy spectrum is always degenerate.

However, there is another natural degeneracy of this spectrum caused by the symmetry of the equilateral triangle. Namely, the same spectrum (60) has solutions which are constructing on the two skeletons *complementing* the considered one. The latter skeletons are just the mirror reflections in the two heights of the triangle coinciding with the two SD's defining the skeleton considered.

All these new solutions can, of course, interfere with the solution (59) and with themselves so when trying to stimulate the corresponding state in a cavity certainly such superposed states will be generated rather than the "pure" states (59).

To isolate, however, the states (59) it is enough to remove one of the three corners of the triangle as it is shown in Fig. 13 (c).

The periodic skeleton corresponding to the periodic orbit shown in Fig. 13 (b) contains eighteen bundles. The length of the orbit is equal to $D = 3\sqrt{7}$, while the wideness of each bundle is equal to $w = \frac{1}{2}\sqrt{\frac{3}{7}}$. Therefore, the GSWF's for this case are linear combinations of the eighteen BSWFs. These are also the projections of one of the two exact solutions which can be obtained on the corresponding LSB.

The LSB is just the cylinder-like band with the radius $\frac{D}{\pi}$ and the length w , so using this correspondence, we get for the energy spectra of the superscar states built on the skeleton considered

$$E_{mn} = \frac{1}{2} \frac{4m^2\pi^2}{D^2} + \frac{n^2\pi^2}{2w^2} = \pi^2 \left(\frac{2m^2}{D^2} + \frac{n^2}{2w^2} \right) = \frac{7}{3}\pi^2 \left(\frac{2}{3}m^2 + n^2 \right) \quad (61)$$

with $n \ll \sqrt{\frac{2}{3}}m$ as the condition of their validity in the equilateral billiards.

5.2. The pentagon billiards

The pentagon billiards were also the subject of intensive studies of both theoretical and experimental [27, 28]. In the latter case, the corresponding pentagon cavities were made of some dielectric media. In the very high frequency region, the corresponding electromagnetic waves form different modes among which the whispering gallery one of Fig. 14 was the most prominent. The other pentagon modes shown in the paper of Lebental *et al.* [28] are more difficult for an identification in terms of the corresponding skeletons also because of different boundary conditions considered by the authors.

Nevertheless, below we will discuss also other pentagon modes of SWF's.

Consider first the simplest one which is defined by the whispering gallery skeleton just mentioned and shown in Fig. 14. It would be quite easy to write the corresponding GSWF's. However, we will limit ourselves by quoting merely the corresponding result for the energy spectrum using the one of the corresponding Möbius-like LSB projected into the pentagon billiards. Namely, we have

$$E_{mn} = \frac{\pi^2}{2} \left(\frac{m^2}{25 \cos^2 \frac{\pi}{5}} + \frac{n^2}{\sin^2 \frac{\pi}{5}} \right),$$

$$n \ll 0,029m, \quad m, n = 1, 2, \dots \quad (62)$$

This spectrum is, of course, degenerate. Note also that in the pentagon (white) center the corresponding GSWF's vanish identically.

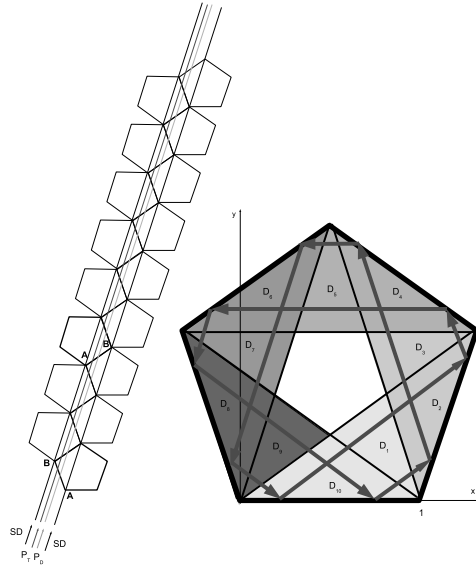


Fig. 14. The pentagon billiard and its simplest whispering gallery superscar skeleton with five bundles. A typical periodic orbit is shown (the straight line P_T in the unfolded pentagon) the limiting form of which is the five-pointed star orbit (the straight lines SD). It degenerates into the inscribed pentagon orbit (the straight line P_D) with the half of the typical period equal to $10 \cos \frac{\pi}{5} \simeq 8.090$. Gluing the end segments indicated by AB in the unfolded pentagon, we get the Möbius band in the phase space.

Another case of the singular skeleton is shown in Fig. 15. The energy spectrum corresponding to the GSWF's built on it is

$$E_{mn} = \frac{\pi^2}{2} \left(\frac{m^2}{(3 \cos \frac{\pi}{10} + 2 \sin \frac{\pi}{5})^2} + \frac{n^2}{\sin^2 \frac{\pi}{10}} \right),$$

$$n \ll 0,076m, \quad m, n = 1, 2, \dots \tag{63}$$

Despite its degeneracy coming from the closed-band form of each periodic skeleton, the spectrum (63) is additionally degenerate by the pentagon rotational symmetry, *i.e.* there are five independent solutions with the same spectrum. In the pentagon cavity, all these solutions can be stimulated simultaneously. To isolate at least one of them it is enough to desymmetrize the pentagon into its forms shown for example in Fig. 16. While by this operation the remaining four modes are not removed, their energy spectra, however, will differ from the modes of Fig. 16.

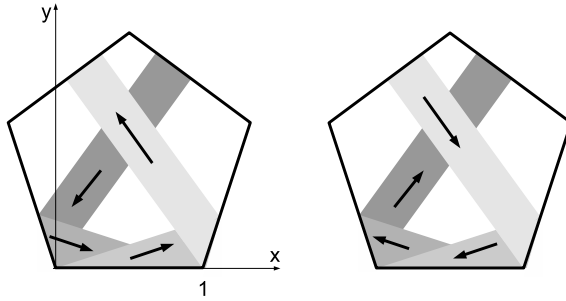


Fig. 15. Another simple singular periodic skeleton in the pentagon billiards with the half of the period equal to $3 \cos \frac{\pi}{10} + 2 \sin \frac{\pi}{5} \simeq 4.029$. Its Lagrange surface is cylinder-like.

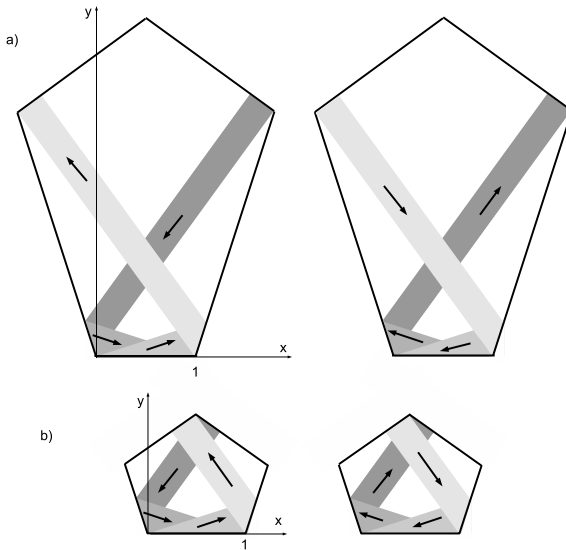


Fig. 16. The deformed pentagon billiards with the singular periodic skeletons having the half periods equal to $2 \cot \frac{\pi}{10} + \cos \frac{\pi}{10} \simeq 7.106$ — the case (a) and $2 \tan \frac{\pi}{10} + 3 \cos \frac{\pi}{10} \simeq 3.503$ — the case (b).

To get the energy spectra for both the cases of the skeletons of Fig. 16, one can consider the LSB's corresponding to the cases to get

$$E_{mn} = \frac{\pi^2}{2} \left(\frac{m^2}{(2 \cot \frac{\pi}{10} + \cos \frac{\pi}{10})^2} + \frac{n^2}{\sin^2 \frac{\pi}{10}} \right),$$

$$n \ll 0,043m, \quad m, n = 1, 2, \dots \tag{64}$$

for Fig. 16 (a), and

$$E_{mn} = \frac{\pi^2}{2} \left(\frac{m^2}{(2 \tan \frac{\pi}{10} + 3 \cos \frac{\pi}{10})^2} + \frac{n^2}{\sin^2 \frac{\pi}{10}} \right)$$

$$n \ll 0,088m, \quad m, n = 1, 2, \dots \tag{65}$$

for Fig. 16 (b).

6. Periodic orbits and superscars in the chaotic polygon based billiards

It follows from the previous section that the idea of the skeletons seems to be effective in solving some simple situations of quantum phenomena related semiclassically with billiards which shapes stimulate rather chaotic than regular (integrable or pseudointegrable) motions. An example of such cases is shown in Fig. 13 (c). Still more spectacular situations exist in billiards which can be obtained from the rectangular and the pentagonal ones by their deformations.

Examples of such deformations and the superscar modes possible to be detected in such chaotic billiards are shown in Fig. 17. To describe analytically the superscar states shown in these figures, the methods of the previous sections can be applied directly.

Note that the superscar mode corresponding to the Sinai billiards of Fig. 17 was observed experimentally by Kudrolli and Sridhar [21] and by Sridhar and Heller [22] who studied the Sinai billiards also numerically (see also [5]).

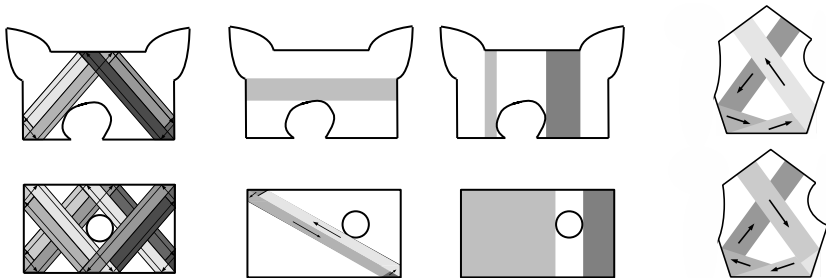


Fig. 17. The deformed rectangular, the Sinai and the pentagon billiards giving rise to chaotic motions with some possible superscar skeletons.

7. Summary and conclusions

In this paper, we have used the Maslov–Fedoriuk approach [15] formulated in terms of the skeletons [13] to construct in the rational polygon billiards singular semiclassical solutions which have forms of the superscar states. The latter have been suggested theoretically by Bogomolny *et al.* [19, 20] and confirmed experimentally by other authors [1, 2, 20–22].

We have shown, in particular, that:

- there is a huge variety of periodic skeletons in the RPB;
- these periodic skeletons continue their existence also in the chaotic deformations of the RPB;
- in the phase space, the Lagrange surface which corresponds to the periodic skeletons in the RPB's have forms of the cylinder-like or Möbius-like bands depending on whether a number of vertices linked by the corresponding SD to close the orbit is even or odd respectively [26];
- the existence of these periodic skeletons gives rise to the appearing of superscar solutions in the RPB's;
- the superscar solutions exist as the exact solutions of the Schrödinger equation on the Lagrange surfaces considered as billiards;
- these exact solutions on the Lagrange surfaces can be considered as the virtual energy levels of the corresponding quantum dynamics of both the RPB and the chaotically deformed RPB manifesting themselves in the high energy limit of this dynamics.

A final conclusion of a more general nature, which can be drawn from our results, is that the periodic orbits seem to play an exceptional role not only in the Feynman paths approach to the quantum mechanics saturating the path integrals [29] but also in the Schrödinger formulation of the quantum mechanics being responsible for the existence of the virtual states in the energy spectra of the billiard dynamics. The well known scar phenomenon of Heller [30], although of a different origin, also suggests such an exceptional role of the periodic orbits in the chaotic dynamics for their quantum description in the language of wave functions.

One of us (S. Giller) would like to express his thanks to prof. P. Kosiński for the suggestion of the meaning of the superscar solutions as the virtual states of the quantum billiard dynamics.

REFERENCES

- [1] S. Sridhar, *Phys. Rev. Lett.* **67**, 785 (1991).
- [2] P.A. Chinnery, V.F. Humphrey, *Phys. Rev.* **E53**, 272 (1996).
- [3] P. Sarnak, *Recent Progress on QUE*, Princeton University and Institute for Advanced Study, September 2009, www.math.princeton.edu/sarnak, unpublished.
- [4] N. Burq, M. Zworski, *SIAM Rev.* **47**, 43 (2005).
- [5] N. Burq, M. Zworski, [arXiv:math/0312098](https://arxiv.org/abs/math/0312098) [math.SP].
- [6] S. Zelditch, [arXiv:math-ph/0503026](https://arxiv.org/abs/math-ph/0503026).
- [7] N. Burq, A. Hassell, J. Wunsch, [arXiv:math/0507020](https://arxiv.org/abs/math/0507020) [math.AP].
- [8] P.J. Richens, M.V. Berry, *Physica* **D2**, 495 (1981).
- [9] S.W. McDonald, A.N. Kaufman, *Phys. Rev. Lett.* **42**, 1189 (1979).
- [10] B. Dietz *et al.*, *Phys. Rev.* **E75**, 035203 (2007).
- [11] P. Sarnak, “The Distribution of Mass and Zeros for High Frequency Eigenfunctions on the Modular Surface”, Dartmouth Spectral Geometry Conference, July 2010, lecture, unpublished.
- [12] S. Tabachnikov, *Student Mathematical Library*, **30**, *Geometry and Billiards*, AMS, 2005,.
- [13] S. Giller, J. Janiak, [arXiv:1108.2527](https://arxiv.org/abs/1108.2527) [math-ph], unpublished; S. Giller, J. Janiak, [arXiv:1301.5212](https://arxiv.org/abs/1301.5212) [math-ph], unpublished.
- [14] H. Mazur, S. Tabachnikov, *Rational Billiards and Flat Structure* in: *Handbook of Dynamical Systems*, Vol. 1A, 2002, pp. 1015–1089, Elsevier Science B.V.
- [15] V.I. Maslov, M.V. Fedoriuk, *Semi-classical Approximation in Quantum Mechanics*, Dordrecht, Boston, London: Reidel, 1981.
- [16] V.I. Arnold, *Mathematical Methods of Classical Mechanics*, Berlin: Springer Verlag, 1978.
- [17] J.B. Keller, S.I. Rubinov, *Ann. Phys.* **9**, 24 (1960).
- [18] M. Boshneritzan, G. Galperin, T. Krüger, S. Troubetzkoy, *Trans. Am. Math. Soc.* **350**, 3523 (1998).
- [19] E. Bogomolny, C. Schmit, *Phys. Rev. Lett.* **92**, 244102 (2004).
- [20] E. Bogomolny *et al.*, *Phys. Rev. Lett.* **97**, 254102 (2006).
- [21] A. Kudrolli, S. Sridhar, *Pramana* **48**, 459 (1997), see also <http://sagar.physics.neu.edu>
- [22] S. Sridhar, E.J. Heller, *Phys. Rev.* **A46**, R1728 (1992).
- [23] E. Bogomolny, C. Schmit, *Nonlinearity* **16**, 2035 (2003).
- [24] L.D. Landau, E.M. Lifshitz, *Quantum Mechanics. Nonrelativistic Theory*, Oxford, New York: Pergamon Press, 1965; A.I. Baz, Y.B. Zeldovich, A.M. Perelomov, *Scattering, Reactions and Decays in Nonrelativistic Quantum Mechanics*, Moscow: Nauka, 1971, in Russian.

- [25] J. Marklof, Z. Rudnick, *J. Spectr. Theory* **2**, 107 (2012).
- [26] L. Halbeisen, N. Hungerbühler, *SIAM Rev.* **42**, 657 (2000).
- [27] E. Bogomolny *et al.*, *Phys. Rev.* **E83**, 036208 (2011).
- [28] M. Levental *et al.*, *Phys. Rev.* **A76**, 023830 (2007).
- [29] M.C. Gutzwiller, *Chaos in Classical and Quantum Mechanics*, Springer, New York 1990.
- [30] E.J. Heller, *Phys. Rev. Lett.* **53**, 1515 (1984).